Available online at www.sciencedirect.com
ScienceDirect
Nuclear Instruments and Methods in Physics Research A 588 (2008) 406–413
NUCLEAR INSTRUMENTS & METHODS IN PHYSICS RESEARCH Section A
www.elsevier.com/locate/nima

The design of a bismuth-based auxiliary filter for the removal of spurious background scattering associated with filter-analyzer neutron spectrometers

T.J. Udovic[a,*], C.M. Brown[a], J.B. Leão[a], P.C. Brand[a], R.D. Jiggetts[b], R. Zeitoun[a,c], T.A. Pierce[b], I. Peral[a,c], J.R.D. Copley[a], Q. Huang[a], D.A. Neumann[a], R.J. Fields[b]

[a]*NIST Center for Neutron Research, National Institute of Standards and Technology, 100 Bureau Dr., MS 6102, Gaithersburg, MD 20899-6102, USA*
[b]*Metallurgy Division, National Institute of Standards and Technology, 100 Bureau Dr., MS 8555, Gaithersburg, MD 20899-8555, USA*
[c]*Department of Materials Science and Engineering, University of Maryland, College Park, MD 20742, USA*

Received 27 November 2007; received in revised form 1 February 2008; accepted 5 February 2008
Available online 17 February 2008

Abstract

The ultimate sensitivity of filter-analyzer-type neutron spectrometers, which are invaluable for measuring the vibrational spectra of materials, is typically limited by spurious background scattering features ubiquitous in all measured spectra. These undesirable features arise from neutrons that are elastically scattered by the sample and then are inelastically scattered by phonon excitations in the beryllium filter material. Such features can be significantly reduced by adding an auxiliary polycrystalline bismuth filter in front of the main filter analyzer. An optimal Bi filter requires a high-purity, low-hydrogen-content material with a sufficiently small crystallite grain size distribution to ensure a sharp Bragg cutoff in the energy dependence of the neutron total cross-section. We were able to produce such a material by the room-temperature compression of dense, high-purity, finely polycrystalline, Bi needles (with an average crystallite grain size of $\approx 230\,\mu m$) synthesized by the rapid water-quenching of melted Bi dripped into a spinning centrifuge. This material resulted in an improved filter performance compared to that using more coarsely polycrystalline Bi synthesized via melt-casting.
Published by Elsevier B.V.

PACS: 29.30.Hs; 29.30.−h; 25.40.Fq; 25.40.Dn; 81.05.−t; 81.20.Ev

Keywords: Bismuth filter; Neutron scattering; Total cross-section; Vibrational spectroscopy

1. Introduction

Filter-analyzer-type neutron spectrometers have been invaluable for characterizing the vibrational density of states (VDOS) of materials for almost a half-century [1–3]. It was recently shown [4] that the spurious background features between 50 and 85 meV (as well as broader and weaker scattering bands above 85 meV) in vibrational spectra measured by these neutron spectrometers were due to phonon excitations of the beryllium filter by neutrons elastically scattered from the sample. It was determined that these features could be significantly reduced by an auxiliary polycrystalline Bi filter placed in front of the main filter. Such a filter could also reduce the thermal- and fast-neutron backgrounds from the sample while only causing a minor attenuation in sample scattering intensity. The original test measurements were performed using a prototype Bi filter with a coarsely polycrystalline morphology (i.e., possessing single-crystal domains with average dimensions of the order of 5–10 mm), typical of the melt-casting process employed. Although a 15 cm thick filter at 100 K was found to be adequate for removing the majority (98%) of spurious background scattering above 50 meV with only a minor (20%) attenuation of the desirable inelastically scattered neutrons below 1.9 meV, it was clear

*Corresponding author. Tel.: +1 301 975 6241.
E-mail address: udovic@nist.gov (T.J. Udovic).

0168-9002/$ - see front matter Published by Elsevier B.V.
doi:10.1016/j.nima.2008.02.006

that a Bi filter with optimized transmission properties should possess a more finely polycrystalline morphology. Yet, the synthesis of such a fine-grained material is nontrivial since it cannot be attained through melt-casting. Rather, it requires more advanced powder-metallurgy techniques. In this paper, we describe our successful search to find the material and procedure necessary to produce such an optimized filter and compare its performance to that of a more coarsely polycrystalline filter synthesized via melt-casting [4].

2. Experimental details

All Bi materials employed came from Belmont Metals or MCP Metal Specialties [5] and had a nominal metals purity of 99.99 at%. Melt-casting and cold-pressing of Bi materials was accomplished with the aid of mild steel molds and dies. Cold-pressing of Bi materials was performed at room temperature using a laboratory-scale, uniaxial hydraulic press for small (3.2 cm diameter) test specimens and an isostatic press at 45 kpsi (0.3 GPa) for larger test specimens. The final Bi morphologies were characterized by normal metallography and basic image analysis using a light microscope.

All neutron measurements were performed at the NIST Center for Neutron Research (NCNR). Hydrogen content of the different Bi starting materials was determined using the neutron prompt-gamma activation analysis (PGAA) instrument [6]. Bismuth transmission measurements were done on the disk-chopper time-of-flight spectrometer (DCS) [7,8] using a pulsed white beam of cold neutrons with 56 μs full-width-at-half-maximum (FWHM) pulse widths, a 10 mm diameter beam cross-section (as defined by a Cd mask), and 30 ms between pulses. The distances from pulse origin and sample position to neutron monitor were ≈2.0 and 0.5 m, respectively. The active cross-section of the neutron monitor was 30 mm wide by 100 mm high. Room-temperature neutron powder diffraction (NPD) patterns for Bi were measured on the BT-1 high-resolution neutron powder diffractometer [9] using 1.5401 Å neutrons from the Cu(3 1 1) monochromator with horizontal divergences of 15′, 20′, and 7′ of arc for the in-pile, monochromatic-beam, and diffracted-beam collimators, respectively.

Bismuth-filter test measurements were made using the filter-analyzer neutron spectrometer (FANS), shown schematically in Fig. 1. A collimated beam of monoenergetic neutrons is extracted from a white beam using a crystalline monochromator (either Cu(2 2 0) or pyrolytic graphite PG(0 0 2)) and directed onto the sample. Some of these neutrons lose energy by exciting vibrational modes in the sample. Before reaching the detectors, these inelastically scattered neutrons must first pass through a low-energy bandpass filter, made up of a 15.2 cm thick polycrystalline graphite layer sandwiched between two polycrystalline beryllium layers (15.2 cm thick in front and 10.2 cm thick in back). The beryllium layers act as better filters than

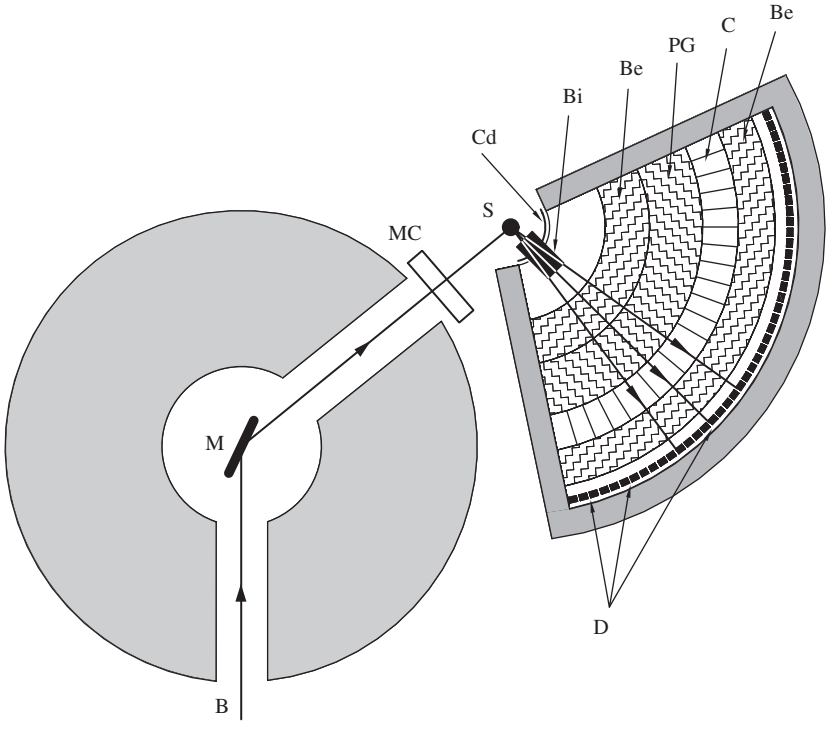

Fig. 1. A schematic diagram of the filter-analyzer neutron spectrometer (FANS) at the NIST Center for Neutron Research, indicating the incident neutron beam (B), monochromator (M), monitor counter (MC), sample (S), Be and pyrolytic graphite (PG) filters, radial and vertical collimators (C), and detectors (D), as described in Ref. [4] and in the text. The location of the additional Bi filter blocks used for spectral tests (see text) is shown in black. The white region in front of the first Be filter layer is intended to house the full Bi filter radial array.

graphite alone for removing the majority of neutrons with energies above 5 meV. The sandwich geometry was chosen since it was empirically shown to reduce more effectively the fast-neutron background, thus leading to an improved signal-to-noise ratio [10]. All the filters are composed of either 5° or 10° wide wedge-shaped sections separated by 1 mm thick ^{10}B–Al alloy absorbing material to capture the unwanted neutrons. Moreover, between the graphite and rear beryllium layers, radial and vertical collimators (with collimations of 5° and 10°, respectively) are used to capture any neutrons not traveling on a line joining the sample with a detector. The composite filter is routinely maintained at a temperature below $\approx$90 K with liquid nitrogen to minimize intensity losses from phonon scattering in the filter materials. It ideally removes all neutrons with final energies above the 1.8 meV Bragg cutoff energy of graphite and results in an average final energy of $\approx$1.2 meV. The composite filter contribution to the total instrumental energy resolution is $\approx$1.1 meV FWHM [11]. Scanning the incident energy yields a scattering spectrum that directly reflects the VDOS of the sample under study, weighted by the neutron cross-sections for the elements in the sample [12].

3. Results and discussion

It was evident from our previous investigation [4] that it was impossible to produce a Bi filter with optimal transmission properties via melt-casting due to the propensity to form unsatisfactorily large crystallites. Therefore, we investigated the powder-metallurgy technique of cold-pressing as a means to obtain a more finely polycrystalline morphology. Four different types of Bi starting materials were investigated: 200, 100, and 8 mesh powders, and rice-size needles synthesized by rapid water-quenching of melted Bi dripped into a spinning centrifuge. Such rapid water-quenching of the latter material inhibited large grain growth. Each material possessed a finer average crystallite grain size than slowly melt-cast Bi. Each material was cold-pressed to $\geqslant$95% theoretical density. Fig. 2 indicates the percentage of theoretical Bi density for each cold-pressed material as a function of the pressure applied. The cold-pressed needles were unique in that they were able to attain close to 100% of the theoretical density under reasonable pressures. Subsequent grain size and porosity analysis by light microscopy involved sample preparation by polishing with up to 1200 grit paper followed by etching in a 1:4 nitric acid/ethanol mixture [13]. Fig. 3 displays the resulting micrographs. A planimetric method was used to determine the average grain size in each case. The 200, 100, and 8 mesh, and needles had average grain sizes of 25, 40, 275, and 230 μm, respectively.

There was concern that the presence of any significant porosity might degrade the transmission properties of a cold-pressed filter by increasing the deleterious effects of small-angle neutron scattering from numerous intergranular pore regions. Hence, to see if sintering could reduce

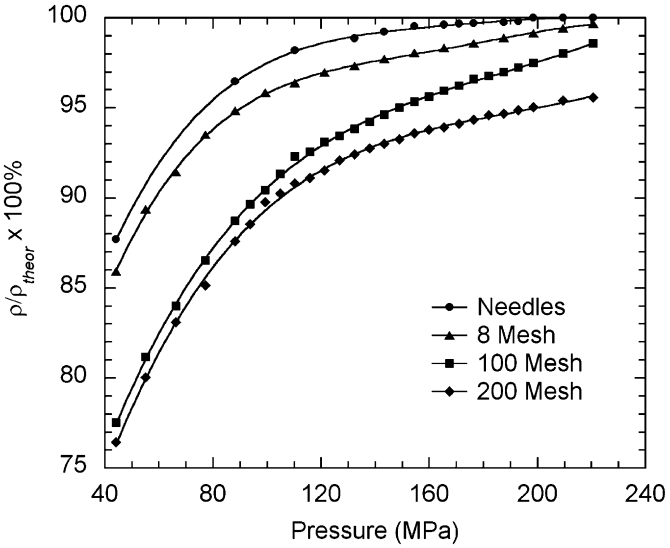

Fig. 2. The ratio of pressed sample density ρ to theoretical Bi density ρ_{theor} vs. applied pressure at room temperature for different Bi starting materials.

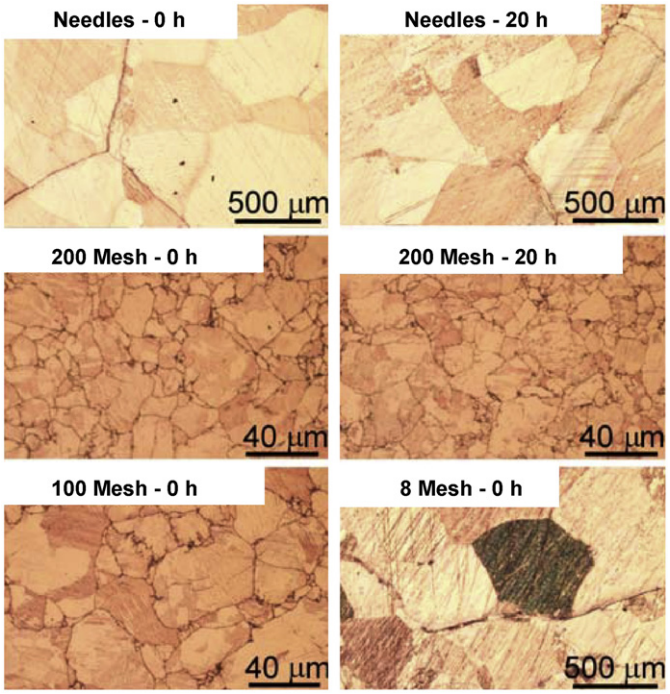

Fig. 3. Grain size micrographs of the different cold-pressed Bi specimens heat-treated in vacuum for various amounts of time. Heat treatments were performed at 523 K, 96% of the Bi melting temperature.

latent porosities without significant increases in crystallite grain size, the cold-pressed specimens were subjected to vacuum annealment at 523 K (96% of the Bi melting point). Resulting micrographs are also displayed in Fig. 3. Fig. 4 plots the average grain size as a function of annealing time. It is evident that, as the time period increases, grain sizes increase significantly for the needle specimen compared to the 200, 100, and 8 mesh powder

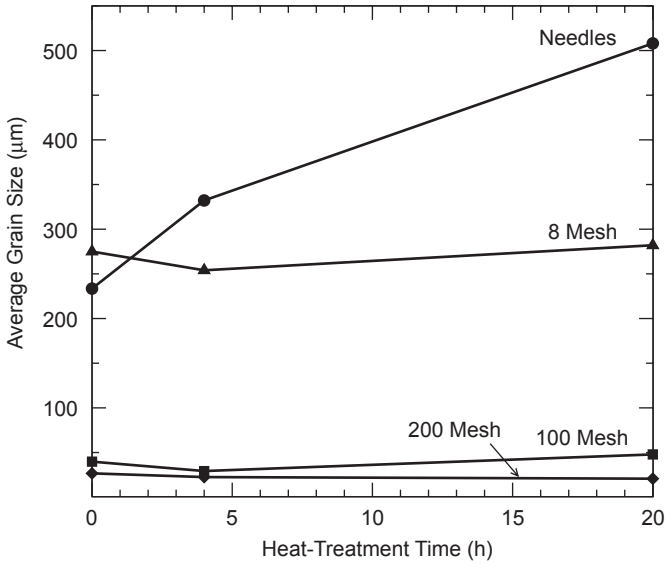

Fig. 4. The effect of the 523 K heat-treatment time on average grain size for cold-pressed Bi specimens made from different starting materials.

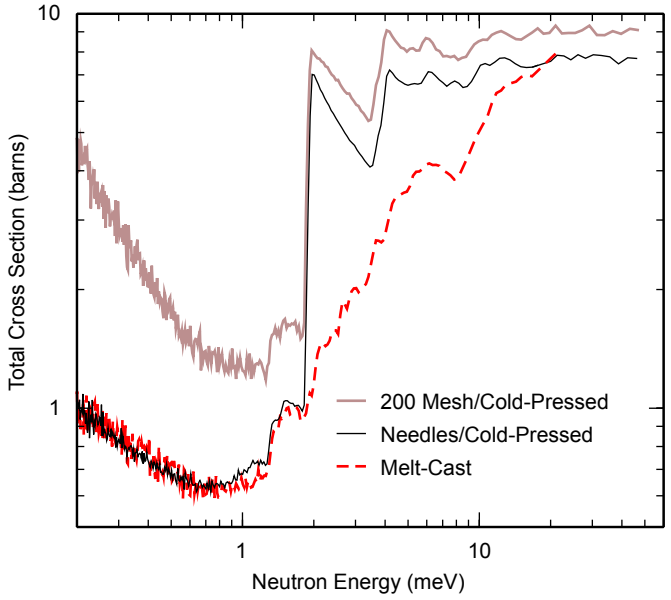

Fig. 5. The neutron energy dependence of the total cross-section at 295 K for cold-pressed Bi synthesized from 200 mesh powder and needles, compared with that of melt-cast Bi. *Note*: 1 barn $= 1 \times 10^{-28}$ m^2.

specimens. This appears to be associated with the lack of intergranular impurities such as oxygen and hydrogen within each needle in contrast to the presence of such impurities on the abundant surfaces of the different mesh powder particles. Such impurities can act as barriers to sintering.

The neutron energy dependence of the total cross-section per atom for each of these Bi specimens was determined from transmission measurements performed on DCS. The transmission, T, for the Bi filter is defined as:

$$T = \frac{I}{I_0} = \exp(-\sigma n t) \tag{1}$$

where I_0 and I are the incident and transmitted neutron intensities, respectively, σ is the total neutron cross-section per atom, n is the atom density, and t is the filter thickness. From this relationship, we can calculate σ from

$$\sigma = \frac{-\ln(T)}{nt}. \tag{2}$$

The resulting total cross-section curves for cold-pressed 200 mesh powders and needles as well as for melt-cast Bi are plotted in Fig. 5. The corresponding curves for cold-pressed 100 and 8 mesh powders are not included for the sake of clarity. In comparison to the melt-cast Bi with its centimeter-sized crystallite domains, all the cold-pressed Bi specimens are found to possess a sharper Bragg cutoff in the total cross-section near 1.9 meV, the result of much smaller average crystallite grain sizes. The cross-section variations among the different cold-pressed specimens is mainly a result of differences in the residual nonmetallic impurity levels, in particular, hydrogen, which has a much larger total cross-section per atom. It is clear that the enhanced total cross-section, especially below 1.9 meV, for the cold-pressed 200 mesh specimen is a reflection of measurable amounts of incorporated hydrogen. This is due to the nature of the starting material, which is composed of porous, high surface area, air-exposed particles. The interaction of surface oxidation and humidity results in particle surfaces decorated with adsorbed hydroxyl groups and water that remain upon cold-pressing. The highest hydrogen content found by PGAA was $\approx$0.5 mol% for the 200 mesh specimen, which had the highest initial surface area. The cold-pressed 100 and 8 mesh specimens had decreasingly lower yet significant hydrogen contents, resulting in total cross-section curves between those of the cold-pressed 200 mesh and needle specimens.

In contrast, the cold-pressed needles have very little associated hydrogen, $\approx$0.06 mol%, because of the much smaller surface areas involved. The combination of extremely low hydrogen content and fine-grained morphology in this case proved to be sufficient for generating an optimal cross-section curve, similar to that in Ref. [14]. This was consistent with the Bi NPD pattern from cold-pressed needles at 295 K. The model refinement was in good agreement with a single phase with the reported R$\bar{3}$m-symmetric Bi structure [15]. Relative peak intensities reflected a complete powder averaging (i.e., no preferred orientation effects) due to the sufficiently large number of randomly oriented crystallite grains in the beam. In contrast, the melt-cast Bi NPD pattern at 295 K [4] possessed relative peak intensities reflective of a significant preferred orientation, which is consistent with the less-defined Bragg cutoff for the total cross-section curve. Nonetheless, the hydrogen content of melt-cast Bi is found to be very low, similar to that of the cold-pressed needles. It should be noted that the melt-cast Bi used in this study was synthesized from different starting material than that used

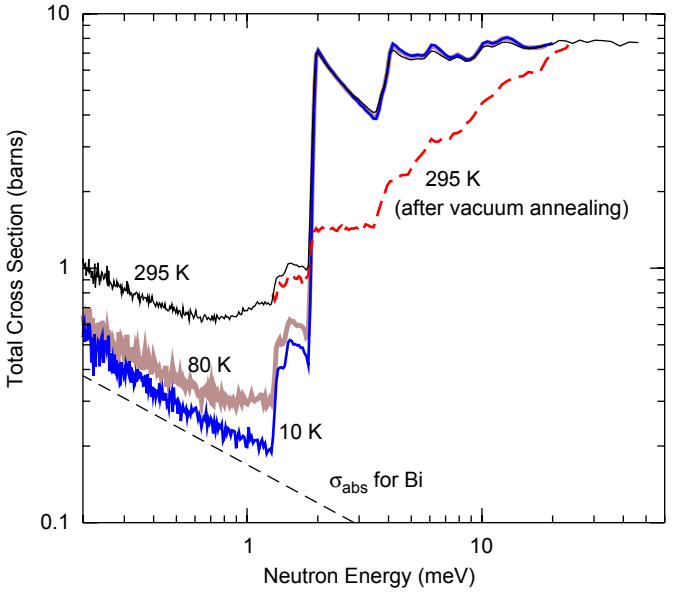

Fig. 6. The neutron energy dependence of the total cross-section for cold-pressed Bi needles as a function of temperature. The dashed line represents the 295 K total cross-section after a 20 h vacuum annealing at 523 K. The absorption cross-section for Bi is included for comparison (assuming a 0.0338 b absorption cross-section for 25 meV neutrons [17]).

in Ref. [4]. The total neutron scattering cross-section curve below 1.9 meV for the melt-cast specimen in the current study (Fig. 5) is somewhat improved compared to the analogous specimen in Ref. [4], the former displaying a cross-section curve $\approx$0.1 b lower than the latter and in good agreement with the curve for the cold-pressed needles. This suggests that the overall purity of the former melt-cast specimen was somewhat lower than expected. Hence, the current melt-cast material should result in slightly higher filter transmissions compared to that reported in the previous study [4], as was found to be the case.

Since the total cross-section curves indicated that the rapidly water-quenched Bi needles were the cold-pressed material of choice, we investigated the effect of room-temperature chemical etching of the needles before cold-pressing to see if we could decrease filter brittleness and/or improve machinability. The Bi needles typically displayed a heterogeneous gray color, reflective of a trace amount of surface oxidation. It was postulated that decreasing or eliminating this trace oxide layer would improve the inter-needle adhesion and improve the structural robustness of the cold-pressed composite. A test batch of needles was etched in a 1:1 hydrochloric acid/water mixture [13] for 10 min followed by multiple rinses in water. This process was repeated once more followed by room temperature vacuum drying. The resulting needles were a more vibrant silver color. Yet, a subsequent cold-pressed specimen seemed to possess the same brittleness and machinability as the specimen made from the unetched needles. Moreover, the total cross-section curves were found to be identical, indicating that the etching process is, for all practical purposes, unnecessary.

Fig. 6 illustrates the effect of a 20 h vacuum annealing at 523 K on the total cross-section at 295 K for cold-pressed Bi needles. It is evident that vacuum annealing is detrimental to the transmission properties. The porosity of cold-pressed needles is already negligible and the main effect of annealing is to increase significantly the average crystallite grain size, thus degrading the sharpness and size of the Bragg cutoff.

The temperature dependence of the total cross-section curve for cold-pressed Bi needles is also illustrated in Fig. 6 along with the neutron absorption cross-section for Bi. The total cross-section is sensitive to temperature only below the Bragg cutoff, since in this region, its magnitude is dominated by neutron scattering from thermally excited Bi phonons and neutron absorption by Bi. As the temperature is decreased, the population of these phonons decreases, and the total cross-section approaches the absorption cross-section. Since the phonon cutoff energy for Bi is relatively low (13.2 meV $\approx$ 153 K) [4,16,17], the data show that the filter transmission below 1.9 meV can be improved significantly by cooling the filter to as low a temperature as practical below 100 K. Previous data [4,14] indicate that the Bi total cross-section below 1.9 meV is independent of morphology. For a 15 cm thick filter, the temperature dependence displayed in Fig. 6 suggests that one can increase the transmission of "desirable" neutrons from nearly 70% at room temperature to $\approx$80% at 100 K and $\approx$85% at 20 K.

Two 15 cm thick test filters, one cold-pressed from needles and one melt-cast, were synthesized for FANS measurements. As in our previous investigation [4], each test filter had a 70×70 mm cross-section and was positioned inside a 70×70 mm square-cross-section Cd tube (with 0.6 mm wall thickness) that was also 15 cm in length (see Fig. 1). The cold-pressed filter was composed of several stacked individual sections while the melt-cast filter was comprised of one piece. The Cd tube acted as an absorber of thermal neutrons scattered by the filter and provided an orifice of constant solid angle for detection of neutrons scattered by the sample. The FANS measurements were performed with both filters at room temperature.

Fig. 7 displays FANS vibrational spectra for the 85.5 meV deuterium optical phonon in $NbD_{0.6}$ at 295 K [18] comparing the results with and without the two Bi test filters above. Fig. 8 displays a similar comparison for polycrystalline V acoustic phonons at 295 K. As discussed in Ref. [4], the addition of the Bi filters removes the Be phonon features above 50 meV, replacing them with a spurious Bi phonon feature at 12 meV (as evident in Fig. 8). The integrated intensities of the measured phonon features using the cold-pressed and melt-cast filters are $\approx$67% and 73%, respectively, of the measured intensities without the filters, thus reinforcing the contention that cooling the Bi filters below 100 K would be beneficial for improving signal

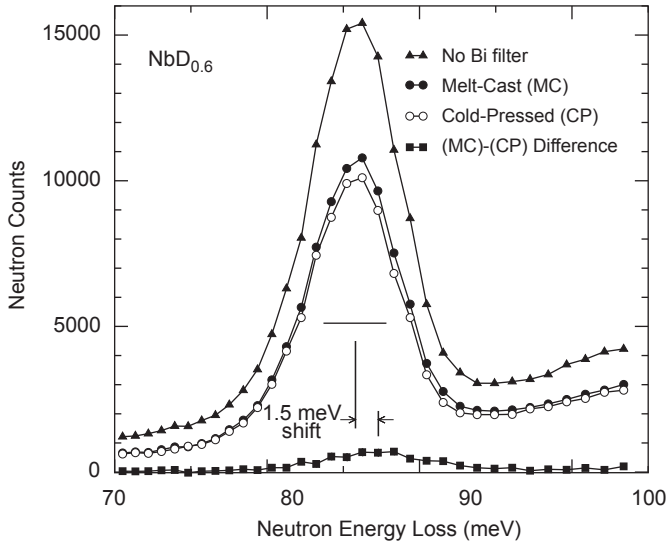

Fig. 7. FANS vibrational spectra for $NbD_{0.6}$ at 295 K for no Bi filter and for 15 cm thick melt-cast and cold-pressed Bi filters. Measurements were done with 60′ and 40′ horizontal collimators, respectively, before and after the Cu(2 2 0) monochromator. The nominal FWHM resolution is depicted by the horizontal bar beneath the spectra. The difference spectrum resulting from the melt-cast-filter spectrum minus the cold-pressed-filter spectrum is clearly shifted upward by ≈1.5 meV compared to the main phonon peak.

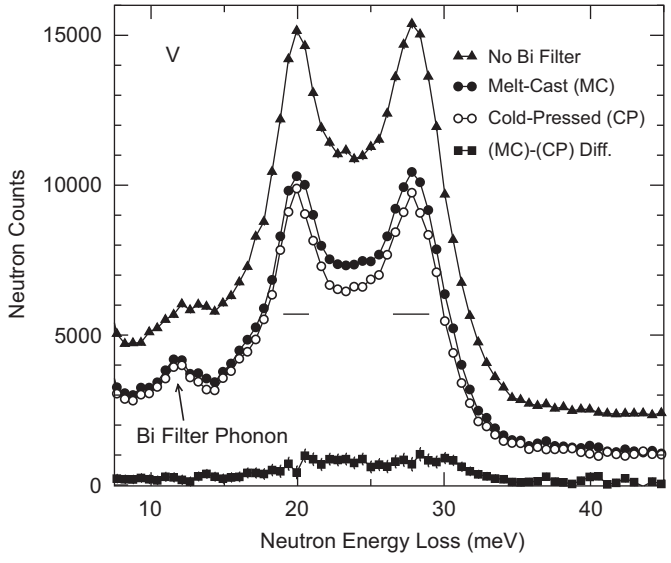

Fig. 8. FANS vibrational spectra for V at 295 K for no Bi filter and for 15 cm thick melt-cast and cold-pressed Bi filters. Measurements were done with 60′ and 40′ horizontal collimators, respectively, before and after the PG(0 0 2) monochromator. The nominal FWHM resolution is depicted by the horizontal bars beneath the spectra. The difference spectrum represents the melt-cast-filter spectrum minus the cold-pressed-filter spectrum.

intensity. As mentioned earlier, the transmission using the melt-cast filter is somewhat higher than observed in Ref. [4], in agreement with the improved total cross-section curve in Fig. 5.

Looking back at Fig. 5, it is clear that the main difference in the total cross-section curves for the two filters is in the region just above the Bragg cutoff energy. It was expected that the sharper cutoff and the relatively larger total cross-section values between 1.9 and ≈10 meV for the cold-pressed filter compared to the melt-cast filter would result in a somewhat enhanced reduction in the leakage of undesirable scattered neutrons in this energy region and a slightly improved instrumental resolution. Figs. 7 and 8 indicate that the difference in this leakage between the two filters is of the order of 8% of the integrated phonon signal. This seems at first glance to be an undesirable loss in measured phonon signal for the cold-pressed filter. Yet, as explicitly pointed out for the difference spectrum in Fig. 7, it is clear that the centroid of the extra leakage intensity using the melt-cast filter is indeed shifted ≈1.5 meV higher in energy than the main phonon signal, indicating that it is comprised totally of undesirable neutrons with final energies above the 1.9 meV Bragg cutoff energy. Since the two existing beryllium filter layers are thick enough to remove the majority of undesirable scattered neutrons above 5 meV, one would expect the observed leakage intensity using the melt-cast filter to originate from neutrons with final energies distributed between 1.9 and 5 meV, with a more significant fraction having final energies closer to the 1.9 meV edge. Hence, the 1.5 meV upward shift observed for the leakage intensity (which translates into an average final energy for these neutrons of $1.2+1.5=2.7$ meV) seems reasonable. Having said this, the surprising effectiveness of the melt-cast filter despite its less-than-optimal filtering properties in this energy region indicates that the existing polycrystalline graphite layer, in addition to the beryllium filter layers' performance, already removes the majority of undesirable scattered neutrons between 1.9 and 5 meV before they can reach the detectors. Nonetheless, the somewhat better filtering properties of the cold-pressed filter compared to the melt-cast filter as well as to no Bi filter indeed translate into a minor improvement in the measured instrumental resolution for the $NbD_{0.6}$ phonon peak near 86 meV in Fig. 7 (i.e., 4.13 ± 0.06 meV FWHM for the cold-pressed filter compared to 4.33 ± 0.06 meV FWHM for the melt-cast filter and 4.38 ± 0.06 meV FWHM for no Bi filter). Since the 8% leakage intensity associated with the melt-cast filter is up-shifted from the true phonon position by 1.5 meV, the improvement in resolution and peakshape for the cold-pressed filter should be somewhat more dramatic for measurements with sharper phonon peaks at lower energies where the instrumental resolution can approach 1 meV FWHM.

Fig. 9 illustrates the fast-neutron background for both the V sample and no sample, with and without the two Bi test filters, indicating that the addition of either filter leads to an identical reduction in the fast neutron background from the sample. Comparing the backgrounds with and without V, it is clear that both Bi filters remove more than

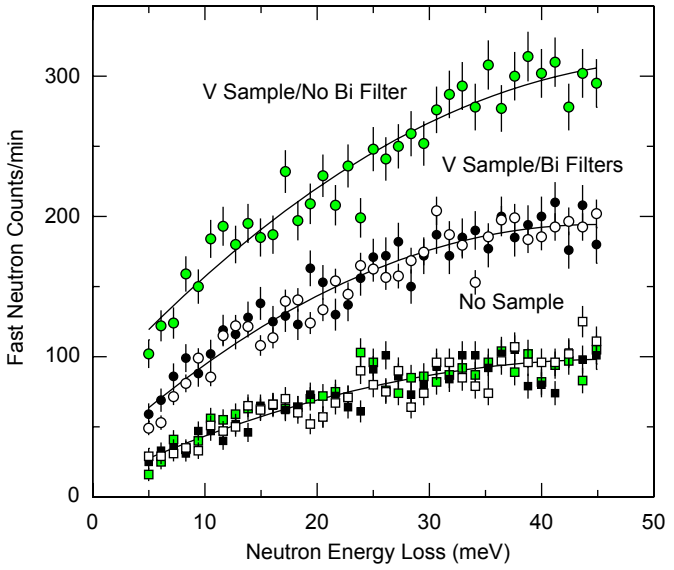

Fig. 9. Total fast-neutron background counts/min vs. neutron energy loss for V at 295 K (circles) compared with that for no sample in the beam (squares): for no Bi filter (shaded symbols), a 15 cm thick melt-cast Bi filter (black symbols), and a 15 cm thick cold-pressed Bi filter (white symbols). Measurements were done with 60′ and 40′ horizontal collimators, respectively, before and after the PG(0 0 2) monochromator and a 0.6-mm-thick layer of cadmium placed in front of the Bi filter assembly described in the text. Error bars represent ±1 S.D. based on counting statistics. Solid lines are least squares quadratic fits to the data.

half of the fast neutrons originating from the sample, as observed previously [4].

4. Conclusions

An optimized polycrystalline Bi filter for filter-analyzer-type neutron spectrometers can be manufactured by cold-pressing finely polycrystalline Bi needles synthesized by rapid water-quenching of melted Bi dripped into a spinning centrifuge. Such a filter possesses a total cross-section curve with a markedly sharper and larger Bragg cutoff at 1.9 meV compared with that of a melt-cast filter. The performance of a cold-pressed filter for neutron vibrational spectroscopy is found to be better than that of a melt-cast filter. Yet, the improvement is minor since the existing polycrystalline graphite and beryllium filter layers already remove the majority of undesirable scattered neutrons above 1.9 meV. In fact, a first-generation, room-temperature, 15 cm thick, melt-cast Bi-filter array recently installed on FANS is now routinely being used to preclude any spurious Be-phonon signal from contaminating the spectroscopic measurements. Nonetheless, to attain optimum performance, we are currently in the process of synthesizing a new cold-pressed Bi-filter array. The manufacture of individual wedges is accomplished by room-temperature isostatic compression of Bi needles in an appropriately shaped mild steel die and requires a rather large isostatic press. The process is shown schematically in Fig. 10.

Temperature-dependent transmission measurements have confirmed that cooling a Bi filter below 100 K, no matter what the morphology, leads to a more dramatic improvement by significantly increasing the transmission of "desirable" neutrons. Hence, our next-generation, cold-pressed, Bi-filter array will also be cryocooled.

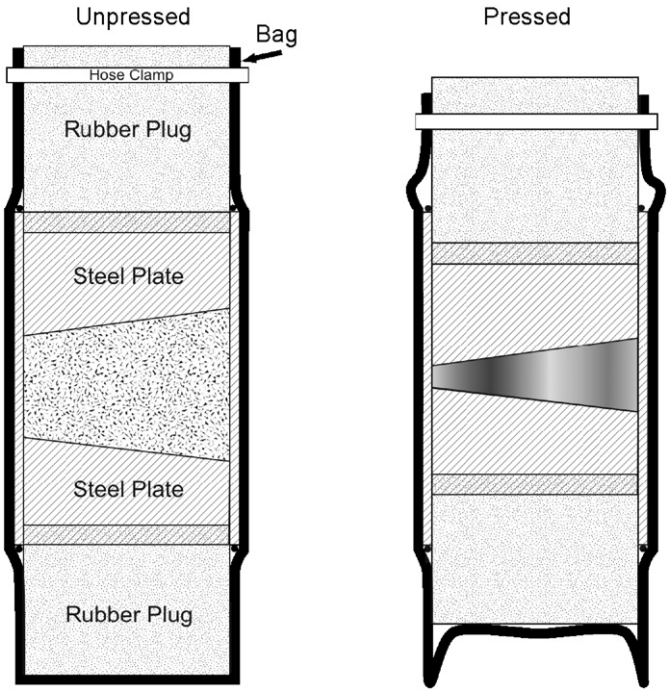

Fig. 10. Schematic of the setup for the manufacture of cold-pressed Bi wedges for the next-generation Bi-filter array.

Acknowledgments

The authors would like to thank J.G. Barker for his assistance with neutron scattering measurements related to this work. This work utilized facilities supported in part by the National Science Foundation under Agreement No. DMR-0454672.

References

[1] B.N. Brockhouse, M. Sakamoto, R.N. Sinclair, A.D.B. Woods, Bull. Am. Phys. Soc. 5 (1960) 373.
[2] B.N. Brockhouse, Inelastic Scattering of Neutrons in Solids and Liquids, IAEA, Vienna, 1961, p. 113.
[3] A.D.B. Woods, B.N. Brockhouse, M. Sakamoto, R.N. Sinclair, Inelastic Scattering of Neutrons in Solids and Liquids, IAEA, Vienna, 1961, p. 487.
[4] T.J. Udovic, D.A. Neumann, J. Leão, C.M. Brown, Nucl. Instr. and Meth. A 517 (2004) 189.
[5] Manufacturers are identified in order to provide complete identification of experimental conditions, and such identification is not intended as a recommendation or endorsement by the NIST.
[6] R.L. Paul, R.M. Lindstrom, Radioanal. Nucl. Chem. 243 (2000) 181.
[7] J.R.D. Copley, T.J. Udovic, J. Res. Natl. Inst. Stand. Technol. 98 (1993) 71.
[8] J.R.D. Copley, J.C. Cook, Chem. Phys. 292 (2003) 477.
[9] J.K. Stalick, E. Prince, A. Santoro, I.G. Schroder, J.J. Rush, in: D.A. Neumann, T.P. Russell, B.J. Wuensch (Eds.), Neutron Scattering in Materials Science II, Material of Research Society Symposium

Proceeding No. 376, Materials Research Society, Pittsburgh, PA, 1995, p. 101.
[10] J.M. Rowe, J.J. Rush, unpublished results.
[11] J.R.D. Copley, D.A. Neumann, W.A. Kamitakahara, Can. J. Phys. 73 (1995) 763.
[12] G.L. Squires, Introduction to the Theory of Thermal Neutron Scattering, Dover Publications, Inc., Mineola, NY, 1996.
[13] G.F. Vander Voort, Metallography: Principles and Practice, ASM International, Materials Park, OH, 1999.
[14] D.J. Hughes, R.J. Schwartz, Neutron Cross Sections, second ed., Brookhaven National Laboratory, 1958 Report No. BNL-325.
[15] D. Schiferl, C.S. Barrett, J. Appl. Cryst. 2 (1969) 30.
[16] J. Sosnowski, S. Bednarski, A. Czachor, Neutrons Inelastic Scattering, vol. I, IAEA, Vienna, 1968, pp. 157–164.
[17] V.F. Sears, Neutron News 3 (3) (1992) 26.
[18] B. Hauer, R. Hempelmann, T.J. Udovic, J.J. Rush, E. Jansen, W. Kockelmann, W. Schafer, D. Richter, Phys. Rev. B 57 (1998) 11115.